ELSEVIER

Journal of Nuclear Materials 265 (1999) 203–207

journal of nuclear materials

Microstructure in Martensitic Steel DIN 1.4926 after 800 MeV proton irradiation

Yong Dai [a,*], Günter S. Bauer [a], Flavio Carsughi [b], Hans Ullmaier [b], Stuart A. Maloy [c], Walter F. Sommer [c]

[a] *Spallation Source Division, Paul Scherrer Institut, CH-5232 Villigen, Switzerland*
[b] *Institut für Festkorpforschung, Forschungszentrum Jülich, 52425 Jülich, Germany*
[c] *APT/TPO, MS H809, Los Alamos National Laboratory, NM 87545, USA*

Received 5 May 1998; accepted 10 August 1998

Abstract

Two double-wall windows of martensitic steel DIN 1.4926 were irradiated with 800 MeV protons at Los Alamos National Laboratory (LANL) to a total number of charged particles of about 6.3×10^{22} protons (2.8 Ah) in a temperature range from 50°C to 230°C. The corresponding maximum fluence at beam centre was of about 2.6×10^{25} p/m^2. Initial examinations on irradiation induced changes of hardness and microstructure have been performed. The preliminary results of microstructural investigation show that precipitates become amorphous after irradiation. There are no evident changes in precipitate size and compositions. Voids and helium bubbles are not observed.

1. Introduction

For spallation neutron sources of a medium or high power ($\geqslant \sim 1$ MW) liquid metal targets are being studied as an alternative to heterogeneously cooled solid metal targets [1]. As there is very little experience on the effects of high energy proton irradiation on mechanical properties of materials, the suitability of austenitic steels and martensitic/ferritic steels as materials for the liquid metal container is being examined based on results of neutron irradiation [2–4]. High energy proton irradiation differs from neutron irradiation in such matters as: (1) a recoil spectrum of much higher energy [5]; (2) high helium and hydrogen production rates [6,7]; and (3) high transmutation rates [7]. Investigation of the behaviour of materials in a realistic spallation radiation environments is therefore essential.

The Pb–Bi liquid metal target concept for the Swiss spallation neutron source (SINQ) at the Paul Scherrer Institut (PSI) dates back to the 1980s [8]. Martensitic stainless steel was chosen for both the Pb–Bi container and the safety window. In order to study the behaviour of the safety window under high energy proton irradiation, two full scale windows were manufactured by PSI and irradiated at LANL [9]. Now the windows are being investigated jointly by Forschungszentrum Jülich (FZJ), PSI and LANL. In the present paper, first results on microstructural changes will be presented.

2. Experimental

The windows were manufactured from the martensitic steel, DIN 1.4926. The composition of this material is in wt%: Fe + 0.20C, 0.36Si, 0.46Mn, 0.019P, 0.006S, 10.5Cr, 0.9Mo, 0.64Ni, 0.26V, 0.009W, <0.01Nb, 0.034Cu, 0.019Co, 0.003Ti. The received material was normalised at 1050°C for 30 min and tempered at 720°C for 1 h. The windows were circular about 200 mm in diameter. Each window consisted of

* Corresponding author. Tel.: +41-56 310 4171; fax: +41-56 310 3131; e-mail: dai@psi.ch

0022-3115/99/$ – see front matter
PII: S0022-3115(98)00505-4

two curved shells with a radius of curvature of 160 mm. The thickness of each shell was 2 mm. There was a 2 mm wide gap between the shells and 40°C cooling water was running through the gap during the irradiation. The outer surfaces of the windows were exposed to air during the irradiation which was performed over 240 days during 1989 and 1990 at LAMPF using 800 MeV protons. The total number of protons received was about 6.3×10^{22} (2.8 Ah). The temperature during irradiation varied from point to point on the windows because of the beam intensity profile; its maximum value at the outer surface in the centre of the beam did not exceed 230°C.

A γ-scan of the radioactivity as a function of position was performed to determine the dose distribution on the window, and it showed a two-dimensional Gaussian distribution with $2\sigma_x = 32.6 \pm 0.2$ mm and $2\sigma_y = 47.2 \pm 0.2$ mm. The maximum fluence at the beam centre is then about 2.6×10^{25} p/m^2, which corresponds to about 6.8 dpa if a displacement cross section of 2600 barns is used [7].

Strips were cut from the window and the one through the centre was used for microstructural investigations and hardness tests. This strip was cut into seven segments each 15 mm long. Segment numbers 1, 3 and 4 were selected for the present study. The fluences at the middle points of these three segments are about 1.5×10^{24}, 1.3×10^{25} and 2.4×10^{25} p/m^2, which correspond to 0.39, 3.4 and 6.2 dpa, respectively.

The segments were ground from 2 mm to about 0.3 mm thickness, then thinned to about 0.15 mm by electro-polishing. 2.3 mm diameter disks were punched from the segments. TEM samples were prepared using an electrolyte of 5% $HClO_4$ + 95% Ethanol electro-polished at −17°C with ~85 V. Samples of unirradiated material were prepared in a similar way.

The observation was performed in a Phillips EM430 microscope equipped with an X-ray energy dispersive spectrometer (EDX). The working voltage was 300 kV.

3. Results

3.1. Microstructures in unirradiated material

A typical view of the structure in the non-irradiated material is shown in Fig. 1. It consists of martensite laths with precipitates located mostly at boundaries. The dislocation density is fairly low in the matrix of subgrains. The size of precipitates varies from about 0.1 to 1 μm. The chemical compositions of precipitates were analysed by EDX. The results from precipitates of relatively large size (>~300 nm) show that the precipitates are rich in Cr (45–65 wt%), and Fe (25–35 wt%), with low Mo, V, Mn, Ni and Si contents. The precipitates in the non-irradiated material are mainly $M_{23}C_6$ type,

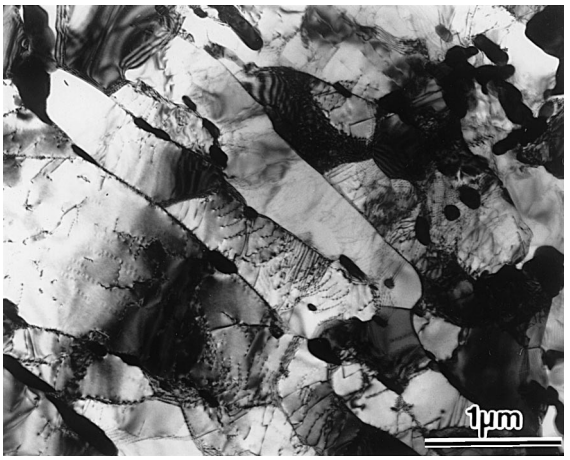

Fig. 1. Microstructures in the unirradiated material.

which is in agreement with observations on 9–12% Cr martensitic steels [10,11].

3.2. Microstructures in irradiated material

There are no evident changes in the appearance of the precipitate structure after irradiation, as can be seen in Fig. 2 which shows an example observed after a dose corresponding to 3.4 dpa. EDX analysis shows that there is no significant change in compositions of the precipitates as compared to those in unirradiated samples. However, the crystal structure of these precipitates has changed significantly: from *crystalline* to *amorphous*.

The observations on samples after 3.4 and 6.2 dpa are essentially the same. Fig. 3 shows a micrograph from a sample of 3.4 dpa. Diffraction patterns taken at two large precipitates in the figure are the same, showing only rings, as illustrated at the upper right corner. This

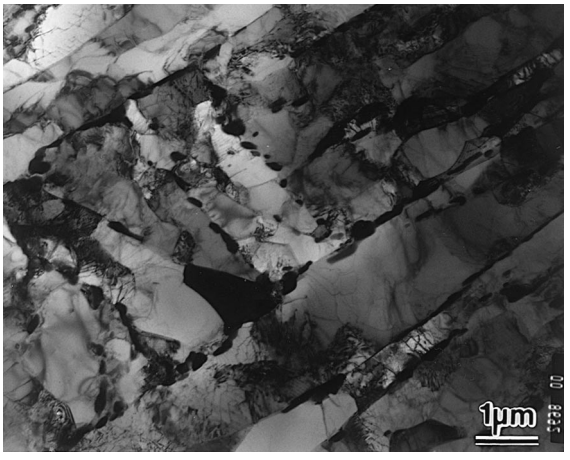

Fig. 2. Microstructures in an irradiated sample of about 3.4 dpa.

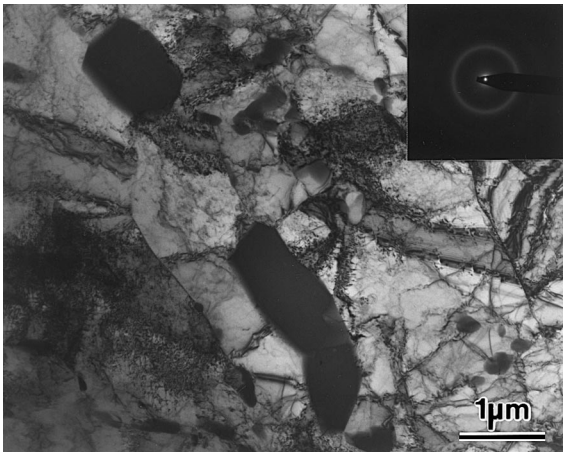

Fig. 3. Micrograph showing precipitates and their diffraction pattern after irradiation to about 3.4 dpa. The diffraction rings indicate the precipitate are amorphous.

shows that these precipitates are completely amorphous. Although nanoprobe technique has not been used, rings could also be clearly seen in the diffraction pattern taken from small precipitates. A dark field image, presented in Fig. 4, indicates that the small precipitates, like the larger ones, are amorphous.

The amorphous transformation starts at low doses. In the samples of 0.39 dpa the transformation has started but not come to completion. This can be seen in Fig. 5. Diffraction pattern 1 was taken from the precipitate indicated by an arrow, and consisted of both spots and rings, as shown in the upper part of Fig. 5(a). The spot pattern demonstrates a fcc crystalline structure, which means the spots are diffracted from the

Fig. 4. Dark field image showing precipitate structures in a sample of 3.4 dpa.

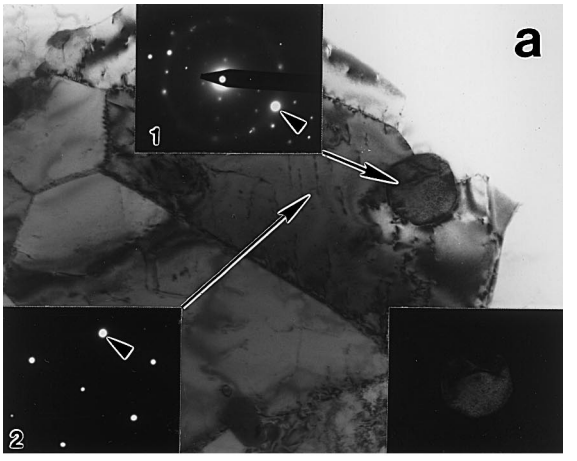

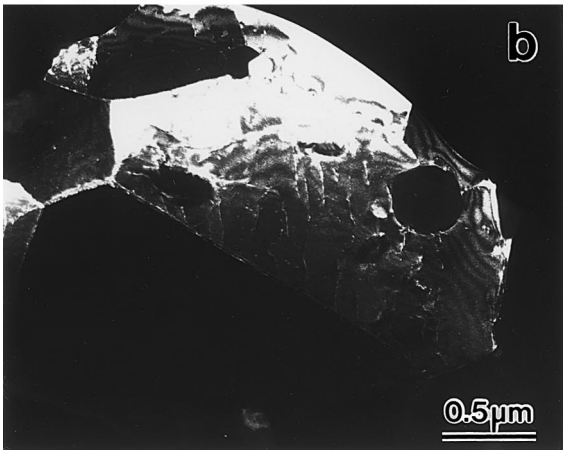

Fig. 5. Micrographs showing bright (a); and dark (b) field image of an area in a sample of about 0.39 dpa. Diffraction pattern 1 from the precipitate shows a complex of spots and a ring (only the first ring is included in this small graph). The dark field images (b); and the small one at the lower right corner of (a) are imaged with the spots indicated in diffraction pattern 2 and 1, respectively.

$M_{23}C_6$ precipitate [12]. The image shown at the lower right corner of Fig. 5(a) is formed with the diffraction spot marked by an arrow in diffraction pattern 1. The bright image of the precipitate on the dark background indicates the crystalline structure of the precipitate. On the other hand, the rings, with the same diameter as that shown in Fig. 3 (camera length is different for the two cases), show the amorphous structure formed in the precipitate. In Fig. 5(b), the dark field image is obtained with the diffraction spot from the matrix indicated in diffraction pattern 2 at the lower left corner of Fig. 5(a), where the dark image of the precipitates also implies that the precipitate is amorphous.

This preliminary investigation shows that dislocation structures in non-irradiated material have changed

substantially following irradiation, which can be seen in Fig. 2. Small dislocation loops produced by irradiation are observed, as shown in Fig. 6 taken from a sample of 6.2 dpa. There are no helium bubbles or voids observed although the calculated He concentration is as high as 600 appm.

4. Discussion

The main result found in this study is a crystalline to amorphous transformation of $M_{23}C_6$ precipitates in martensitic steel DIN 1.4926 irradiated with 800 MeV protons at temperatures of about 230°C and below. The amorphization can be already observed at a dose as low as 0.39 dpa and appears to be complete at 3.4 dpa. At the lower dose of 0.39 dpa, the amorphous structure is found coexisting with crystalline structure in the same precipitate.

The changes in precipitate structures in martensitic steels with 8–12% Cr induced by neutron [10,11,13] and ion (of low energy) [14,15] irradiation at temperatures above 300°C have been well studied. There, new precipitate phases produced by irradiation have been observed. However the amorphization of the initially present precipitates has not been noticed. The present irradiation differs from the above irradiations in two main aspects: (1) 800 MeV protons generate much higher energy recoil spectra and much higher transmutation rates, especially for helium and hydrogen. The consequences of this are difficult to assess at present; (2) the irradiation temperature is lower, $\leqslant 230$°C, especially in the low dose regions. Similar phenomena observed in zirconium alloys [16,17] suggest that the irradiation temperature plays a more important role.

The amorphization of precipitates observed in the present work might be explained in a similar way as that proposed by Naguib and Kelly [18] for radiation induced amorphization in intermetallics. Namely, the amorphization can take place during irradiation when the ionicity (degree of ionic interatomic bonding) is smaller than 0.4, and the crystallization temperature (T_C) for the amorphous phase is greater than 0.3 T_{ma} (T_{ma}, the absolute melting point temperature for the amorphous phase). If the T_C for the amorphous precipitates in this material is between 200°C and 300°C (0.3 T_m corresponds to about 250°C for martensitic steels), one can attribute the amorphization to the temperature effects, i.e., as the irradiation was performed at temperatures $<T_C$, therefore the amorphization induced by irradiation can remain. On the other hand, for those irradiations performed at temperatures $\geqslant 300$°C, which is higher than T_C, the amorphous structures are crystallised spontaneously during irradiation.

Since the irradiation temperature is low, <0.3 T_m, segregation processes enhanced by irradiation should be slow. Consequently, the initial precipitate structures should be difficult to change and the new precipitate phases might be difficult to form. This may be the reason for no evident changes in the compositions and morphology of the precipitates observed. The lack of observable He bubbles and voids is likely due to the low irradiation temperature.

The present study will be continued in detail in future and will determine the mechanism for the amorphization of the precipitate structures and also on the quantitative analysis of irradiation induced dislocation loops. In parallel, mechanical properties tests are proceeding, which will show any impact that the amorphous precipitate structures have on the mechanical properties of martensitic steels.

Fig. 6. Bright field image showing small dislocation loops formed during irradiation.

5. Conclusions

1. Amorphization of precipitates was observed in martensitic steel DIN 1.4926 irradiated with 800 MeV protons at temperatures $\leqslant 230$°C. In samples at a dose of $\geqslant 3.4$ dpa, the precipitates are completely amorphous. In samples at a dose of about 0.39 dpa, the precipitates show both crystalline to amorphous structure.
2. The compositions of precipitates and the appearance of precipitate structures in irradiated samples are similar to those in non-irradiated samples.
3. There are no He bubbles or voids observed.

Acknowledgements

The authors thank Dr W. Kesternich for useful discussions and Mr H. Derz and T. Floßdorf for preparing the samples.

References

[1] G.S. Bauer, Proc. of the 13th Meeting of the Int. Collaboration on Advanced Neutron Sources (ICANS-XIII) and Fourth Plenary Meeting of the European Spallation Source Project (ESS-PM4), PSI-Proceedings 95-02, 1995 p. 547.
[2] Y. Dai, Proc. 13th Meeting of the Int. Collaboration on Advanced Neutron Sources (ICANS-XIII) and Fourth Plenary Meeting of the European Spallation Source Project (ESS-PM4), PSI-Proceedings 95-02, 1995, p. 604.
[3] K. Farrell, L. Mansur, Proc. of Int. Workshop on Spallation Materials Technology, Oak Ridge, Tennessee, 1996, p. 3.3-1.
[4] H. Ullmaier, F. Carsughi, Nucl. Instrum. Methods B 101 (1995) 406.
[5] M. Victoria, M. Alurralde, A. Caro, A. Horsewell, S. Proennecke, Mater. Sci. Forum 97–99 (1992) 541.
[6] S.L. Green, W.V. Green, F.H. Hegedus, M. Victoria, W.F. Sommer, B.M. Oliver, J. Nucl. Mater. 155–157 (1988) 1350.
[7] M. Wechsler, M.H. Barnett, D.J. Dudziak, L.K. Mansur, L.A. Charlton, J.M. Narnes, J.O. Johnson, in Materials for Spallation Neutron Sources, The Minerals, Metals, and Materials Society (TMS), Warrendale, PA, 1999, p. 23.
[8] G.S. Bauer, Proc. 11th Meeting of the Int. Collaboration on Advanced Neutron Sources (ICANS-XI), KEK-Report 90-25 (1991) 41.
[9] M. Dubs, J. Ulrich, Proc. 11th Meeting of the Int. Collaboration on Advanced Neutron Sources (ICANS-XI), KEK-Report 90-25 (1991) 524.
[10] P.J. Maziasz, R.L. Klueh, J.M. Vitek, J. Nucl. Mater. 141–143 (1986) 929.
[11] C. Hsu, D.S. Gelles, T.A. Lechtenberg, Proc. 13th Int. Symp. on Radiation Induced Changes in Microstructure, ASTM STP 955, Philadephia, 1987, p. 545.
[12] W. Kesternich, Radiat. Eff. 78 (1983) 261.
[13] D.S. Gelles, G.L. Hankin, M.L. Hamilton, J. Nucl. Mater. 251 (1997) 188.
[14] P. Jung, J. Nucl. Mater. 179–181 (1991) 745.
[15] J. Kai, G.L. Kulcinski, R.A. Dodd, Proc. 13th Int. Symp. on Radiation Induced Changes in Microstructure, ASTM STP 955, Philadelphia, 1987, p. 530.
[16] R.W. Gilbert, M. Griffith, G.J.C. Carpe, J. Nucl. Mater. 135 (1985) 265.
[17] W.J.S. Yang, R.P. Tucker, B. Cheng, R.B. Adamson, J. Nucl. Mater. 138 (1986) 185.
[18] H.M. Naguib, R. Kelly, Radiat. Eff. 25 (1975) 1.